J. Chem. Sci. © Indian Academy of Sciences.
DOI 10.1007/s12039-016-1188-8

Structure of N′-(adamantan-2-ylidene)benzohydrazide, a potential antibacterial agent, in solution: Molecular dynamics simulations, quantum chemical calculations and Ultraviolet–visible spectroscopy studies

ALEXANDER M ANDRIANOV[a], IVAN A KASHYN[a], VIKTOR M ANDRIANOV[b], MAKSIM B SHUNDALAU[c,*], ANTON V HLINISTY[c], SERGEY V GAPONENKO[b,c], ELENA V SHABUNYA-KLYACHKOVSKAYA[b], ANNA MATSUKOVICH[b], ABDUL-MALEK S AL-TAMIMI[d] and ALI A EL-EMAM[e]

[a]Institute of Bioorganic Chemistry, National Academy of Sciences of Belarus, 5/2 Kuprevich Str., 220141, Minsk, Belarus
[b]B.I. Stepanov Institute of Physics, National Academy of Sciences of Belarus, 68 Nezależnaści Ave., 220072, Minsk, Belarus
[c]Physics Department, Belarusian State University, 4 Nezależnaści Ave., 220030, Minsk, Belarus
[d]Department of Pharmaceutical Chemistry, College of Pharmacy, Salman Bin Abdulaziz University, Alkharj 11942, Saudi Arabia
[e]Department of Pharmaceutical Chemistry, College of Pharmacy, King Saud University, Riyadh 11451, Saudi Arabia
e-mail: shundalov@bsu.by

MS received 22 July 2016; revised 16 September 2016; accepted 30 September 2016

Abstract. The molecular dynamics simulations of the structure of the *N′*-(adamantan-2-ylidene)benzohydrazide followed by the quantum chemical calculations at the DFT level of theory have identified four stable conformers of this potential antibacterial agent in solution: one "central" *cis*- and three ("central", "left" and "right") *trans*-conformers. The UV-Vis absorption spectrum in the 220–320 nm region in the ethanol solution reveals two bands that can be primarily explained based on the *ab initio* calculations of the spectral characteristics of the "side" *trans*-conformers at the MRPT level of theory. However, the close energy values for the calculated *cis*- $S_1 \leftarrow S_0$ and "side" *trans*- $S_2 \leftarrow S_0$ transitions cannot exclude the presence of *cis*-conformer in solution. Therefore, the data obtained show that the coexistence of both *trans*-conformers and *cis*-conformer should be taken into consideration when studying the pharmaceutical properties of the title molecule.

Keywords. *N′*-(adamantan-2-ylidene)benzohydrazide; UV-Vis spectrum; molecular dynamics simulations; DFT calculations; multi-reference perturbation theory calculations; conformers.

1. Introduction

The insertion of an adamantyl fragment into the structure of some molecules leads to compounds with relatively high hydrophobicity. It can modify the biological activity of these molecules. Usually, an adamantane-containing compound will be more lipophilic than the analogue which does not contain an adamantyl moiety. Through various mechanisms adamantyl fragment positively modulates the therapeutic index of many compounds.[1,2] Derivatives of adamantane are known for their antiviral activity against Influenza A[3–5] and HIV viruses.[6–8] Several adamantane derivatives are also associated with antimicrobial[9–14] and anti-inflammatory activities.[14–16]

The title compound (*N′*-(adamantan-2-ylidene) benzohydrazide, or AYBH, $C_{17}H_{20}N_2O$) was synthesized among a series of *N′*-(adamantan-2-ylidene)aroylhydrazides,[17] which displayed potent broad-spectrum antibacterial activity. However, the mechanism of this activity of the AYBH is uncertain. The coexistence of the different conformers may have a dominant role in biological activity. In order to explore the mechanism of the antibacterial activity of the title compound and its related derivatives, herein the structure of AYBH in solution is studied in detail.

AYBH consists of an aromatic ring and adamantine nucleus connected by a bridge of three atoms including double bond (dihedral angle α_4), amide bond (α_2) and

*For correspondence

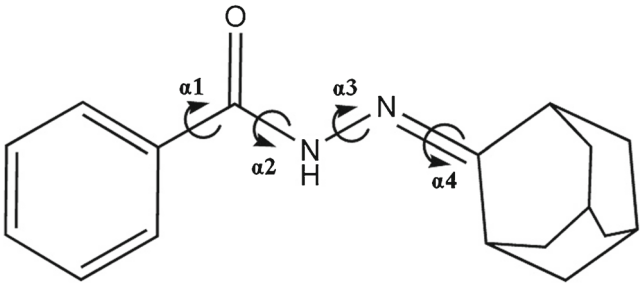

Figure 1. Two-dimensional structure of the title molecule. Dihedral angles are shown by circled arrows.

two single bonds (α_1 and α_3) (Figure 1). The aromatic ring and the adamantine nucleus are conformationally stable and rotation around double bond is hindered. Conformational rearrangements of the molecule may appear by change of the dihedral angles α_2 and α_3 (and possibly α_1). Thus, the title molecule can exhibit several equilibrium configurations in dilute solutions and in the absence of steric distortions.

In the crystal structure,[17] the AYBH molecules are linked *via* N–H$\cdots$N hydrogen bonds. There are also C–H$\cdots$O, C–H$\cdots$N and C–H$\cdots\pi$ interactions within the chains. Based on the IR and Raman spectra and the DFT calculations, we have recently shown[18] that two preferable isomers (*trans*- and *cis*-isomers for C=O and N–H bonds) of the AYBH may appear in crystalline phase. Based on the data of a study,[18] the *trans*- and *cis*-isomers correspond to the α_2 angle of about 180° and 0°, respectively. The X-ray study[17] predicts the *trans*-isomer as the more stable one for the crystalline structure. According to the calculations,[18] the energy of the *trans*-isomer is 9.2 kJ/mol greater than the energy of the *cis*-isomer. The *trans*-isomer is more polar (5.13 D) than the *cis*-isomer (4.29 D), and the electric dipole moment of the *trans*- isomer is oriented rather along the C=O and N–H bonds, while the electric dipole moment of the *cis*-isomer is oriented rather along the C–N and N=C bonds.[18] Thus, it is assumed that for the crystalline structure, an "open" configuration of the chain of the *trans*-isomers is more favorable. In this case each of the *trans*-isomers connects with two (or more) of its neighbors.

To get an insight into the conformational features of the AYBH molecule in solutions, its X-ray structure[17] was subject to molecular dynamics simulations followed by the quantum chemical calculations at the density functional theory (DFT) and multi-reference perturbation theory (MRPT) approximations. The findings obtained were used for the interpretation of the UV-Vis spectrum of AYBH in ethanol.

Time-dependent density functional theory (TDDFT) is currently widely used to model electronic spectra of polyatomic systems.[19–22] It is known[19] that typical quantum chemical calculations using the hybrid functional B3LYP in terms of the TDDFT approximation display deviations of the excited state energies from the available experimental values coming up to 0.4 eV. Moreover, the presence of carbonyl and phenyl groups and the heteroatom (N) in AYBH allows one to classify it as a molecular system that may exhibit the intramolecular charge transfer (ICT). In particular, aniline[23] and benzaldehyde[24] are the examples of such compounds. The phenyl group acts as the acceptor in the former (one of the possible reasons for this relates to the donor property of the amine itself) and as the donor, in the latter. It is also known[25–29] that methods for calculating of electronic spectra based on a local density approximation (even taking into account gradient corrections) in terms of TDDFT are not always able to correctly predict the spectral and energy characteristics of the excited electronic states of the molecular systems with intra- and intermolecular charge transfer (for example, common sources of errors have been comprehensively analyzed in a study[27]). One needs to note that this fundamental inadequacy of the local density approximation does not appear for all molecular systems with ICT. In general, this situation is characteristic of the DFT calculations.[30]

As opposed to the excited states, the geometric structure parameters of the ground state of organic compounds are predicted by DFT methods with the high accuracy.[30] This enables one to use the data of the DFT calculations of molecular structures as the basis for the calculations of UV-Vis spectra at a higher level of theory.

Ab initio calculations of spectral and energetic characteristics of the excited electronic states for the complex molecular system are often performed in such approximations as CASSCF/MRCI (Complete Active Space Self-Consistent Field/Multi-Reference Configuration Interaction), CASSCF/MRCC (Multi-Reference Coupled Clusters), or CASSCF/MRPT (Multi-Reference Perturbation Theory).[31] A new approach to the MS-MR-PT (Multi-State Multi-Reference Perturbation Theory) level of theory, which is called XMCQDPT (Extended Multi-Configuration Quasi-Degenerate Perturbation Theory), which is free from some disadvantages of the earlier versions of the MS-MR-PT, has been developed by Granovsky.[32] Recently,[33] we have shown that the *ab initio* calculations at the CASSCF/XMCQDPT2 (Extended Multi-Configuration Quasi-Degenerate 2nd Order Perturbation Theory)[32] level of theory predict the spectroscopic parameters of the ground and some excited states of the KRb molecule with the high accuracy.

In this study, the above quantum chemical methods were used in conjunction with molecular dynamics simulations as described in section 2.2.

2. Experimental and Computational

2.1 *UV-Vis Spectra*

The electronic absorption spectrum of solution of AYBH in ethanol was measured by a Cary 500 (Varian) spectrophotometer. Since the main absorption bands lie in the near ultraviolet range, care has been taken to minimize contribution from the solvent. For this reason, a cell with the solvent was used in the reference channel during measurements to ensure correct subtraction of solvent contribution. Experimental results are shown in Figure 2. The ethanol solution shows the presence of the two absorption bands: long-wavelength band at 280 nm and short-wavelength band at 248 nm. The band positions were determined using fitting of two Gaussian contours.

2.2 *Molecular dynamics simulation*

Molecular dynamics (MD) simulation of the X-ray three-dimensional structure of the title molecule,[17] AYBH was performed using Amber 11[34] with the implementation of the generalized Amber force field.[35] Hydrogen atoms were added to the crystal structure[17] by the xleap procedure of AMBER 11.[34] The molecule was solvated using ethanol as an explicit solvent and simulated in an octahedron box with periodic boundary conditions. The ethanol potential was constructed with the Antechamber program in Amber 11[34] using the generalized Amber force field.[35] The system was first energy minimized by 500 steps of steepest descent algorithm followed by 500 steps of conjugate gradient method. Harmonic restraints with force constant of 1.0 kcal/mol were then imposed on the atoms of the system and heating it from 0 to 310 K was carried out over 1 ns at constant volume. Additional equilibration was performed over 1.0 ns by setting the system pressure to 1.0 atm and by using a weak coupling of the system temperature to a 310 K bath[36] with a 2.0 ps characteristic time. In the next stage, all the restraints were removed, and the structure was balanced again at 310 K over 2 ns. Finally, the isothermal-isobaric MD simulation (T = 310 K, P = 1.0 atm) was performed during 60 ns time domain. A Langevin thermostat with collision frequency of 2.0 ps^{-1} and a Berendsen barostat with 2.0 ps characteristic time[34] were used to maintain temperature and pressure, respectively. A simple leapfrog integrator[34] with 2.0 fs time step was used. The non-bonded cut-off distance was set at 8 Å. All bonds with hydrogen atoms were restrained by the SHAKE algorithm.[37] Electrostatic interactions were calculated by the particle mesh Ewald method.[38]

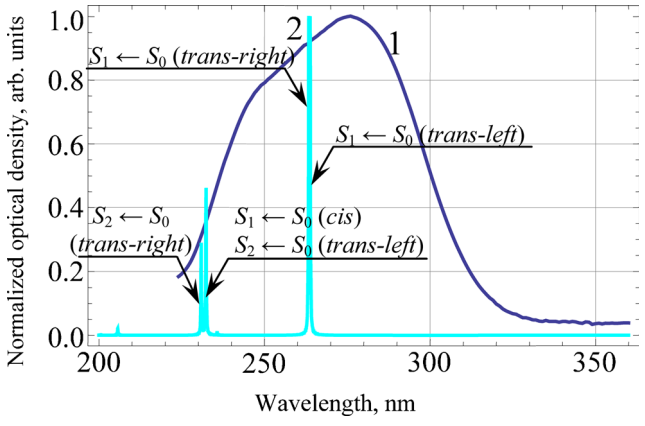

Figure 2. The experimental absorption spectrum of AYBH in ethanol (1) and the absorption bands calculated at the CASSCF(2,8)/XMCQDPT2 level of theory (2).

2.3 *DFT calculations*

The structural analysis of the most probable conformers of AYBH was carried out by the GAMESS-US[39,40] quantum chemical package. The obtained results were visualized by the MacMolPlt[41] program. All calculations were performed using the standard cc-pVDZ basis set[42] by DFT methods using the hybrid B3LYP functional.[43–45] The influence of solvent (ethanol) was taken into account in the approximation of the Polarizable Continuum Model (PCM). The full geometric optimization without any constraints was carried out for each probable conformer. Analysis of the calculated Hessian matrices testifies to the absence of imaginary frequencies, confirming the stability of the conformers. The scans of the potential energy surface along the α_2 and α_3 angles were carried out with the step of 20°. An appropriate angle was fixed and others geometric parameters optimized without other constraints.

2.4 *CASSCF/XMCQDPT2 calculations*

The CASSCF/XMCQDPT2 calculations for the AYBH were performed using the Firefly[46] quantum chemical package with the standard cc-pVDZ basis set.[42] Firstly, the CASSCF calculations with the state-averaged (SA) procedure were done. The active space for the CASSCF calculations was two electrons in eight orbitals. The SA-CASSCF(2,8) procedure was realized for singlet and triplet states. Finally, the calculations for singlets

and triplets were performed at the XMCQDPT2[32] level of theory. All seventy-one lowest double occupied orbitals were included in the perturbation based calculation. The recommended[46] value of the ISA shift (0.02) was used in present approach.

3. Results and Discussion

3.1 *Molecular dynamics simulations*

Conformational flexibility of the title molecule was examined in terms of root-mean-square deviations (RMSD) of atomic coordinates between its MD structures and the first structure of the MD trajectory.[34] At the same time, only the heavy C, N and O atoms were used. The RMSD value versus time for the molecule in ethanol is plotted in Figure 3. Analysis of this figure shows that the structure of the molecule does not undergo considerable changes within the 60 ns time domain. The RMSD values averaged over all the MD structures are 0.8 ± 0.5 Å and 1.5 ± 0.8 Å for the *trans*- and *cis*-conformer, respectively. However, inspection of Figure 3 allows one to reveal two novel conformational states for the conformers of interest that differ in the value of the α_3 angle. The time dependences of dihedral angles of the title molecule for the *trans*-conformer are presented in Figure 4. The data obtained for the *cis*-conformer are close to those for the *trans*-conformer. The average values of dihedral angles for the *trans*-conformer are $\alpha_1 = 179.97 \pm 8.11°$, $\alpha_2 = 179.89 \pm 10.51°$, $\alpha_4 = 180.03 \pm 10.55°$, $\alpha_3 = 94.48 \pm 17.55°$ and $\alpha_3 = 264.74 \pm 19.36°$. The corresponding values for the *cis*-conformer are $\alpha_1 = 179.91 \pm 10.36°$, $\alpha_2 = 0.04 \pm 17.41°$, $\alpha_4 = 179.93 \pm 10.25°$, $\alpha_3 = 98.19 \pm 22.45°$ and $\alpha_3 = 261.77 \pm 22.4°$.

The MD structures of AYBH clustering in the dihedrals space (α_1, α_3) are shown in Figure 5. With the data of this figure, we identified two structural clusters for each conformer. The first cluster was that containing the MD structures with the α_3 angle that did not exceed 180°, whereas the second one was that containing the structures with the α_3 angle that did exceed 180°. According to this criterion, the cluster occupation was evaluated. For the *trans*-conformer, the occupation of the first cluster ($\alpha_3 = 94.48 \pm 17.55°$, *trans-left*-conformer) is 50.4%, and this value for the second one ($\alpha_3 = 264.74 \pm 19.36°$, *trans-right*-conformer) is 49.6%. The RMSD value between the structures equals to 4.50 Å. For the *cis*-conformer, the occupation of the first cluster ($\alpha_3 = 98.19 \pm 22.45°$, *cis-left*-conformer) is 49.0%, and for the second one ($\alpha_3 = 261.77 \pm 22.4°$, *cis-right*-conformer) it comes to 51.0%. The RMSD value between the structures equals to 5.34 Å.

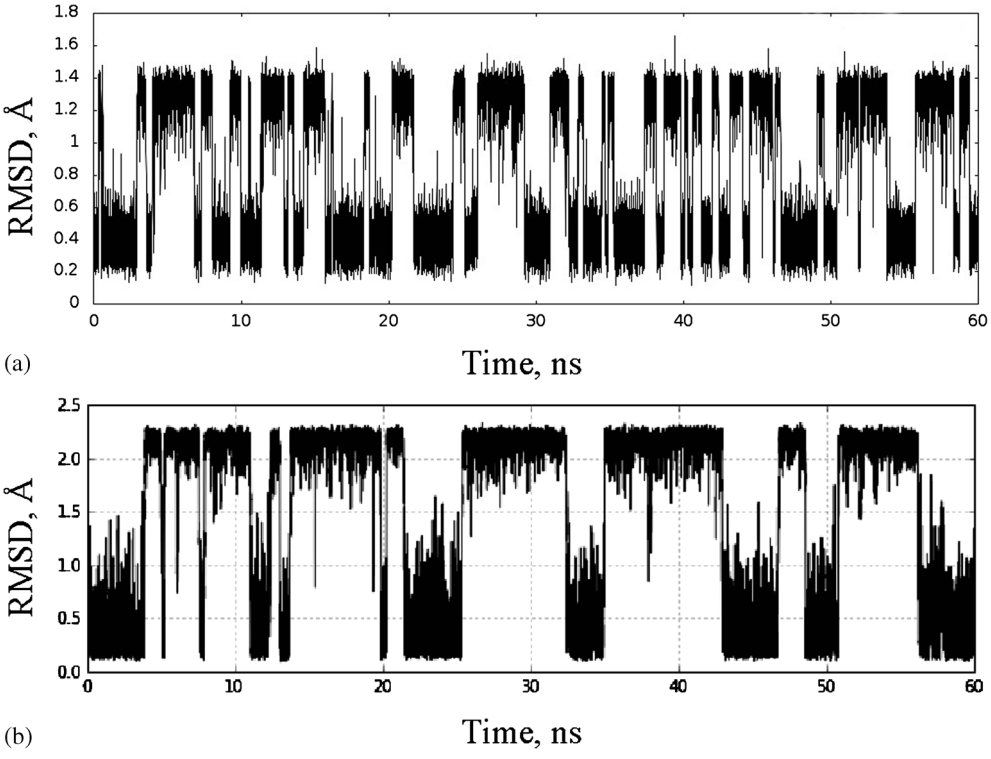

Figure 3. Time dependence of the RMSD of atomic coordinates between the MD structures and the first MD trajectory structure for the *trans*- (*a*) and *cis*-conformer (*b*) of the title molecule in ethanol.

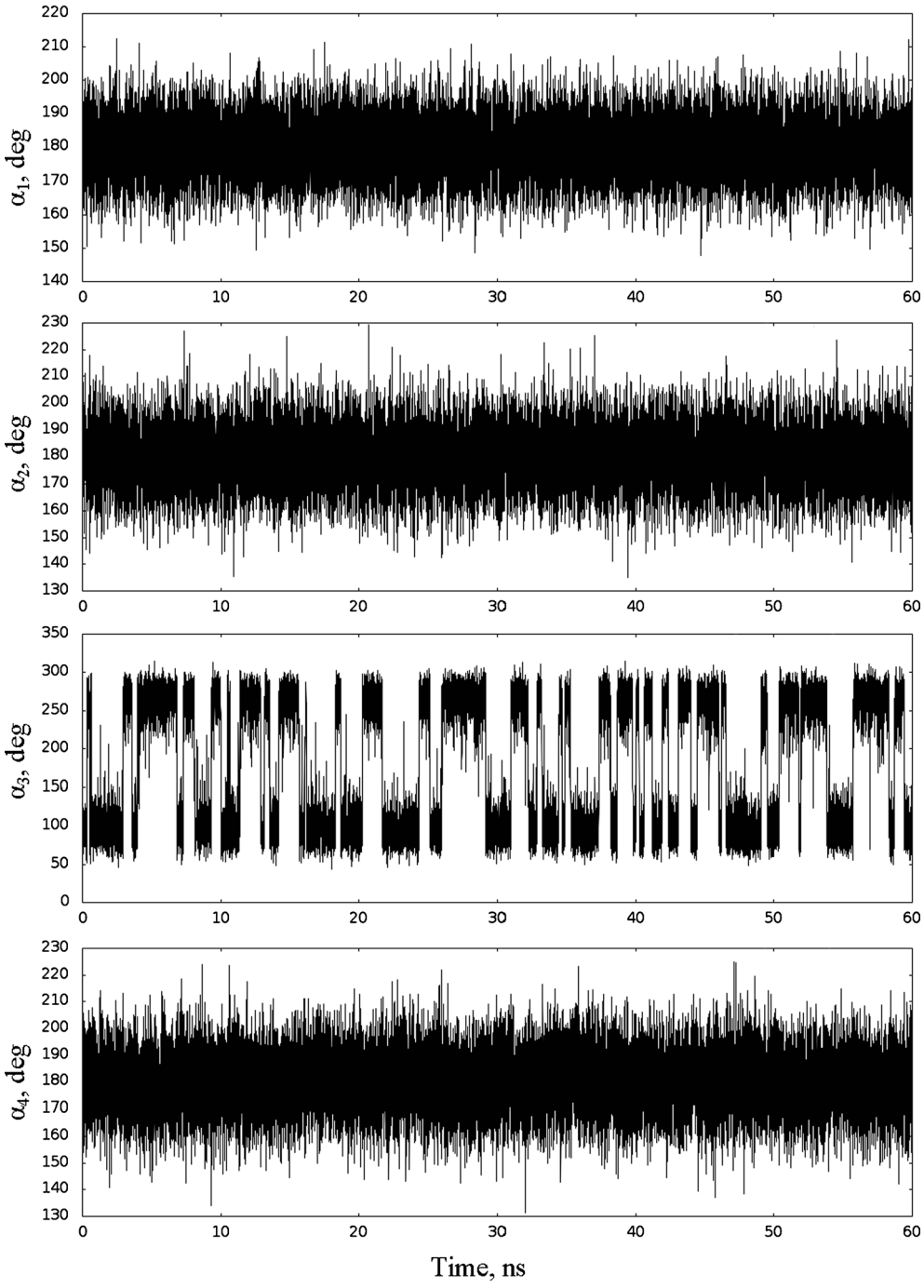

Figure 4. Time dependencies of dihedral angles for the *trans*-conformer of the title molecule in ethanol.

Figure 6 casts light on the structures of AYBH in the above clusters superimposed with matching of the aromatic ring. Analysis of this Figure indicates that, both in *trans*- and *cis*-conformation, AYBH changes in dynamics only the spatial orientation of the adamantine nucleus relative to the aromatic ring, the orientation being defined by the α_3 angle.

Clustering the MD trajectory over atomic coordinates was performed by the Means method using the RMS distance metric.[34] Based on the angle analyses, the MD trajectory was divided into two clusters for each conformer. For the *trans*-conformer, two clusters were found with the following parameters: (i) occupation value is 50.3%, the average distance to the centroid being 0.316 Å; (ii) occupation value is 49.7%, the average distance to the centroid being 0.317 Å. The RMSD value between the structures equals to 3.90 Å. For the *cis*-conformer, two clusters were found with the following parameters: (i) occupation value is 49.0%, the average distance to the centroid being 0.377 Å;

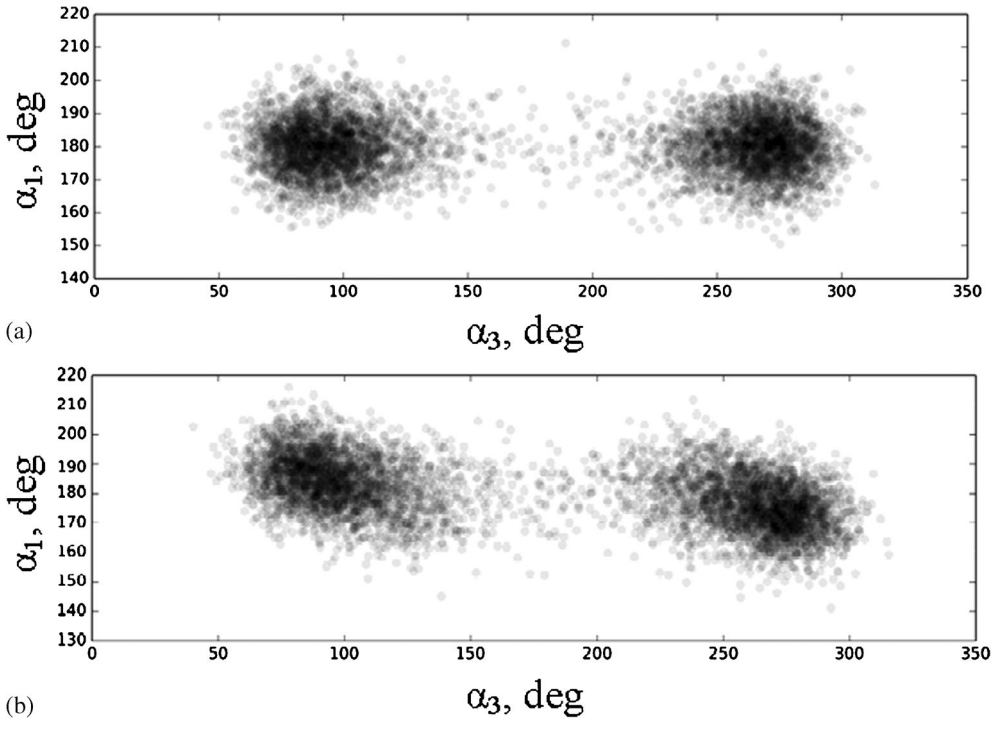

Figure 5. MD structures for the *trans*- (*a*) and *cis*-conformer (*b*) of AYBH in ethanol clustering over α_1 and α_3 angles.

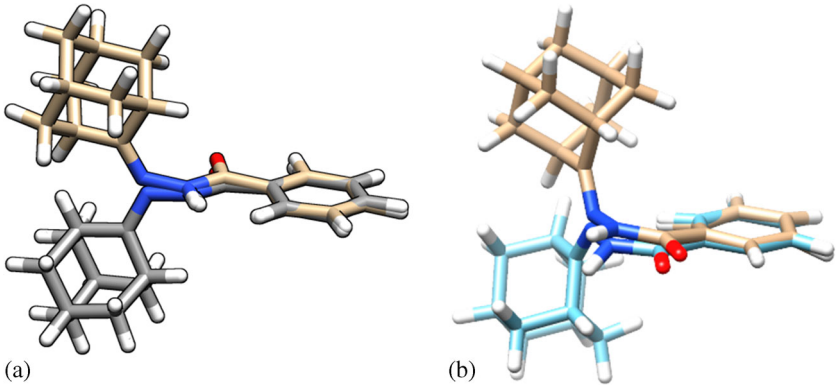

Figure 6. Superimposed structures of the identified clusters for the *trans*- (*a*) and *cis*-conformer (*b*) of the title molecule in ethanol. The structures are the closest to those with geometric parameters averaged over all the conformers of clusters 1 and 2.

(ii) occupation value is 51.0%, the average distance to the centroid being 0.377 Å. The RMSD value between the structures equals to 5.94 Å.

The data on the dihedral angles for every representative structure of the conformers of AYBH in ethanol resulting from clustering the MD trajectory over dihedral angles and atomic coordinates are cited in Table 1.

3.2 *DFT calculations*

So the DFT calculations[18] and MD simulations predict six possible conformers of the title molecule. Two conformers presenting *trans*- and *cis*-isomers of the molecule were previously detected by the DFT methods.[18] In these conformers, the α_3 angle is close to 180°, and the α_2 angle is approximately 180° and 0° for *trans*- and *cis*-isomers respectively.[18] In addition, the MD simulations reveal for these configurations two probable conformers that may appear in the two "side" versions: the *left*-conformer with the α_3 angle varying from 95° to 98° and the *right*-conformer with the α_3 angle varying from 264° to 261°. At the same time, the DFT conformers[18] are not stable within the MD simulations.

To refine the above structures, the potential energy surface of the title molecule was scanned along the

Table 1. Dihedral angles for the *trans*- and *cis*-conformers of the title molecule in ethanol obtained by clustering the MD trajectory over angular and Cartesian coordinates.

	Clustering type	Cluster number	Dihedral α_1 angle, deg	Dihedral α_2 angle, deg	Dihedral α_3 angle, deg	Dihedral α_4 angle, deg
Trans-conformer	Over coordinates	1	182.71	181.54	94.90	177.91
		2	175.65	175.67	282.12	175.36
	Over angles	1	180.32	180.67	93.81	179.07
		2	179.84	179.57	266.30	179.23
Cis-conformer	Over coordinates	1	181.32	11.54	93.22	178.11
		2	176.15	−14.80	257.55	180.20
	Over angles	1	179.99	0.36	98.29	179.67
		2	179.70	0.94	261.82	180.34

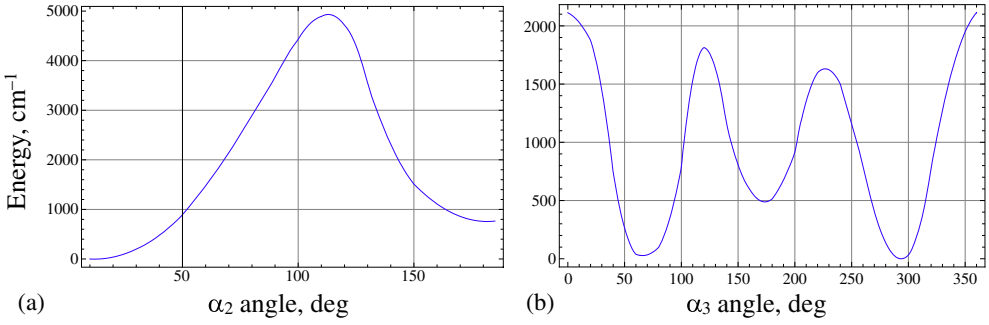

Figure 7. The PEC of the title molecule as a function of the α_2 angle (*a*) and the PEC of the *trans*-conformer as a function of the α_3 angle (*b*) at B3LYP/cc-pVDZ level of theory.

Table 2. Dihedral angles and relative energies for the conformers of AYBH calculated at the B3LYP/cc-pVDZ+PCM level of theory.

Conformer	Dihedral α_1 angle, deg	Dihedral α_2 angle, deg	Dihedral α_3 angle, deg	Dihedral α_4 angle, deg	Relative energy, kJ/mol
Cis	151.00	0.00	182.20	180.0	2.81
Trans	159.14	168.54	186.89	180.0	0
Trans-left	163.17	155.29	70.31	180.0	8.16
Trans-right	−161.15	−155.03	249.43	180.0	8.09

α_2 angle with the step of 20°. The calculated potential energy curve (PEC) is shown in Figure 7*a* in which the minima at 0° and 180° correspond to the *cis*- and *trans*-isomers, respectively. To detect the "side" configurations of the *trans*- and *cis*-isomers, the potential energy surface was scanned along the α_3 angle with the step of 20°. For the *trans*-isomer, the calculated PEC (Figure 7*b*) shows three minima located at 65°, 180° and 295°. The first and the third minima relate to the "side" configurations. For the *cis*-isomer, the "side" configurations were not found. In this case, the PEC displays within the α_3 angle ranges of 40° to 90° and of 320° to 240° rather plateaus with slopes toward the α_3 value of 180°.

One should underlay that the minima of the calculated PECs are not equivalent and potential barriers for the *cis-trans* and *left-center-right* conversations under the normal conditions are too high, suggesting that the AYBH molecule may exist in solution as an equilibrium mixture of different conformations.

In the next point of the DFT calculations, the equilibrium structures of the conformers of interest were identified at the B3LYP/cc-pVDZ+PCM level of theory based on a full geometric optimization. Dihedral angles and relative energies of the design conformers are cited in Table 2, and their equilibrium structures are shown in Figure 8. According to the data of Table 2 and Figure 8, the presence of solvent results in the additional stabilization of the *trans*-isomer.

Thus, four stable conformers of the AYBH molecule were identified at the B3LYP/cc-pVDZ+PCM level of theory: one "central" *cis*-conformer and three *trans*-conformers associated with the "left", "central" and "right" configurations (Figure 8). The frontier molecular

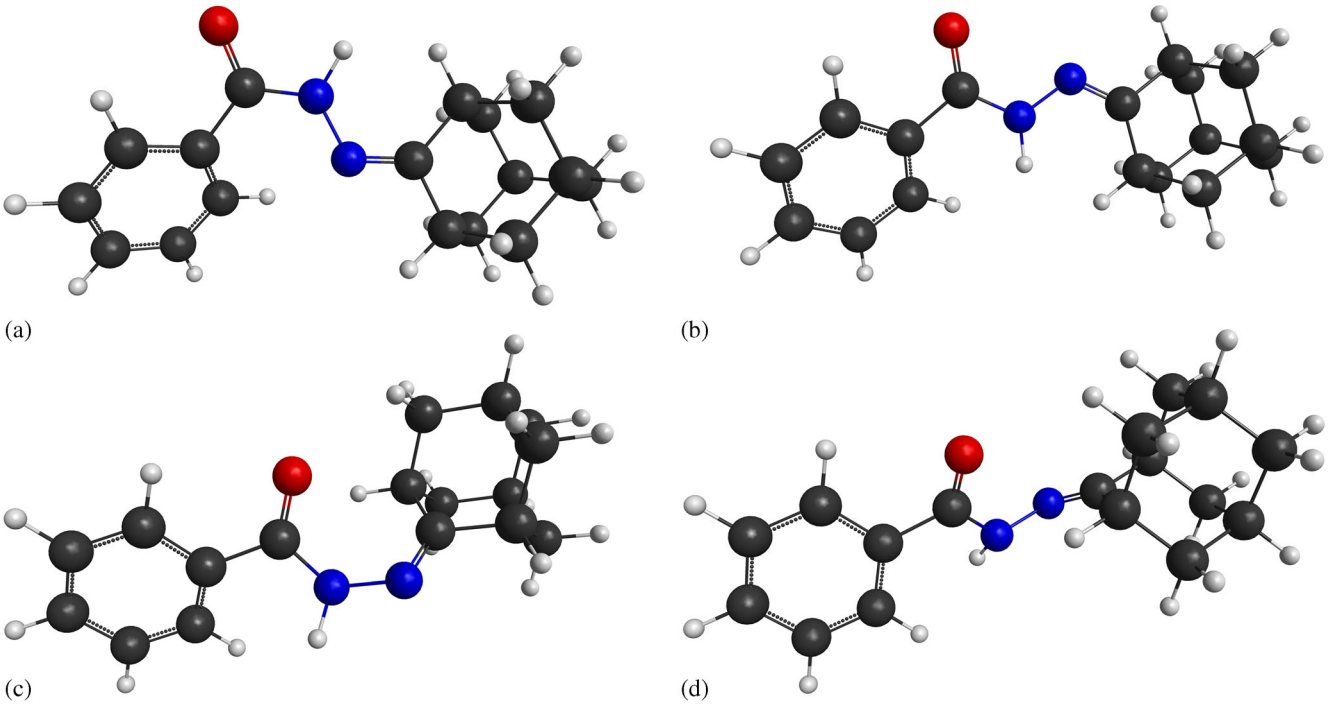

Figure 8. The equilibrium structures of the conformers of the title molecule calculated at the B3LYP/cc-pVDZ+PCM level of theory: (*a*) *cis*-, (*b*) *trans*-, (*c*) *trans-left*- and (*d*) *trans-right*-conformations.

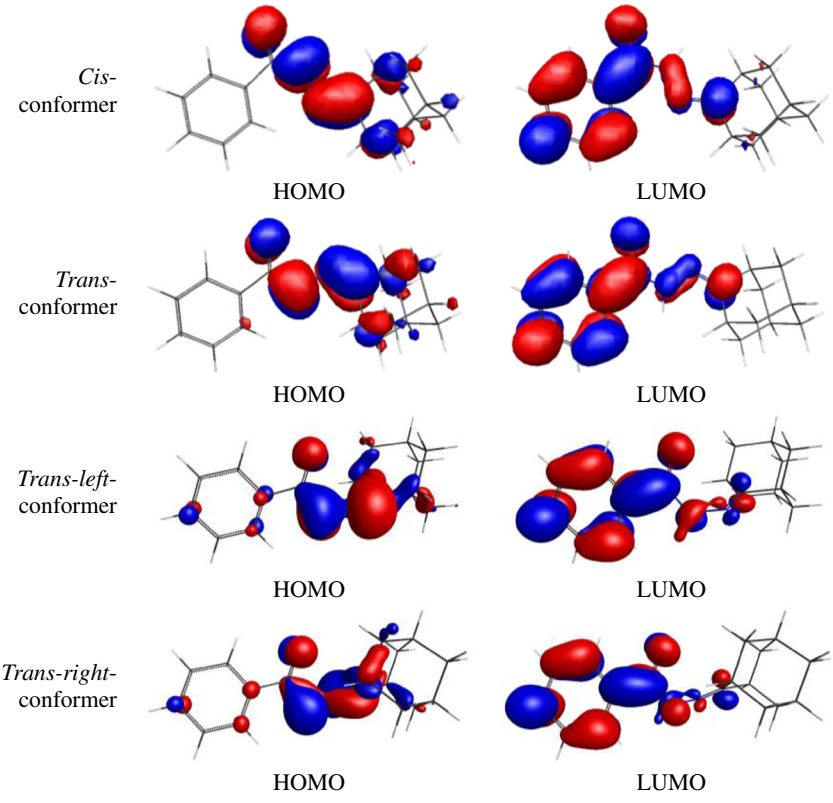

Figure 9. The HOMO and LUMO for the conformers of the title molecule at the B3LYP/cc-pVDZ level of theory.

orbitals (HOMO and LUMO) for these conformers are presented in Figure 9. All the identified conformers demonstrate the ICT features, and therefore, *ab initio* multi-reference methods should be used to calculate their contributions to the electronic absorption spectrum of AYBH (see Introduction section).

Table 3. Spectral characteristics for the lowest electronic states of the conformers of AYBH calculated at the CASSCF(2,8)/XMCQDPT2 level of theory.

Conformer (Boltzmann's weight)	Singlet states				Triplet states		
	S_n	Relative energy, cm^{-1}	λ ($S_n \leftarrow S_0$), nm	Transition dipole ($S_n \leftarrow S_0$)	T_n	Relative energy, cm^{-1}	λ ($T_n \leftarrow S_0$), nm
Cis (0.060)	0	426					
	1	43477	232	2.255	1	31010	327
	2	49049	206	0.714	2	43191	234
Trans (0.002)	0	1127					
	1	43560	236	2.260	1	31910	325
	2	51014	200	0.880	2	44642	230
Trans-left (0.470)	0	0					
	1	37914	264	1.705	1	30802	324
	2	43040	233	0.939	2	39095	256
Trans-right (0.468)	0	1					
	1	37975	263	1.711	1	30714	326
	2	43315	231	0.942	2	39361	254

3.3 *CASSCF/XMCQDPT2 calculations*

Finally, the equilibrium configurations of AYBH optimized by the B3LYP/cc-pVDZ+PCM procedure were subject to the calculations at the CASSCF(2,8)/XMCQDPT2 level of theory. The results of these calculations obtained for the lowest singlet and triplet states are given in Table 3. As compared to the B3LYP/cc-pVDZ+PCM calculations, the CASSCF(2,8)/XMCQDPT2 level of theory predicts greater stability for the "side" conformers: *trans-left*- and *trans-right*-conformers exhibit the minimal values of energy. We suppose that it is caused by different contributions of the excited configurations to the ground state for these conformers. The DFT calculations describe only non-excited electronic configuration and, therefore, allow one to derive for each conformer a certain distribution of the electron density and the total energy. In contrast to DFT, the CASSCF/MRPT level of theory is a multi-configuration method taking into consideration contributions of the excited configurations to the ground state. These contributions are unique and determined by the structural features of the conformer.

The "side" conformers exhibit the long-wavelength $S_1 \leftarrow S_0$ transition at 264 nm and $S_2 \leftarrow S_0$ transition at 232 nm (Table 3). For both "central" conformers, the $S_1 \leftarrow S_0$ transition is in the same spectral range (near 235 nm). The differences in the values of the $S_1 \leftarrow S_0$ excitation energy for the "side" and "central" conformers may be caused by different positions of the adamantyl moiety relative to the molecular "frame", leading to the difference in the values of the transition moments and their orientations relative to the molecular coordinate axes. For the "central" conformers, the transition moments have significant x- and y-components (the x axis is directed along the long axis of the molecule). In the case of the "side" conformers, the x-component is considerably greater than the y-component. The absorption bands calculated for these conformers are presented in Figure 2.

Taking into account (i) possible deviation of calculated versus experimental values of the transition energies, (ii) the Boltzmann's weight of each conformer, and (iii) long-wavelength shifts due to polar solvent (ethanol) effect, one can suggest that the experimental long-wavelength band (280 nm) contains contributions from the "side" conformers $S_1 \leftarrow S_0$ transitions and the experimental short-wavelength band (248 nm) contains contributions from the "side" conformers $S_2 \leftarrow S_0$ transitions and the "central" conformers and $S_1 \leftarrow S_0$ transitions (see Table 3 and Figure 2). It is worth mentioning that both calculated groups of bands (near 264 and 232 nm) have identical systematic short-wavelength shift of about 16 nm with respect to the experimental bands (280 and 248 nm).

4. Conclusions

The systematic conformational analysis of the *N′*-(adamantan-2-ylidene)benzohydrazide, AYBH, a potential antibacterial agent, was carried out by molecular dynamics simulations and quantum chemical calculations at a high level of theory. The calculations identify four stable conformers of AYBH: one possible *cis*- and three possible *trans*-conformers, whereas the UV-Vis absorption spectrum in the 220–320 nm exhibits two absorption bands in ethanol. Despite the "side" *trans*-conformers explaining satisfactorily the experimental data, the presence of the *cis*-conformer and the "central" *trans*-conformer cannot be excluded because of the very close energy values for the *cis*- and "central"

trans- $S_1 \leftarrow S_0$ transition and the "side" *trans*- $S_2 \leftarrow S_0$ transitions. Therefore, the coexistence of different conformers in solution should be taken into account when analyzing the pharmaceutical properties of the title molecule.

Acknowledgements

Abdul-Malek S. Al-Tamimi and Ali A. El-Emam would like to extend their appreciation to the Deanship of Scientific Research at King Saud University for funding this study through the research group project No. PRG-1436-23.

References

1. Lamoureux G and Artavia G 2010 *Curr. Med. Chem.* **17** 2967
2. Liu J, Obando D, Liao V, Lifa T and Codd R 2011 *Eur. J. Med. Chem.* **46** 1949
3. Hayden F G 2006 *Antiviral Res.* **71** 372
4. Pérez-Pérez M-J, Balzarini J, Hosoya M, De Clercq E and Camarasa M-J 1992 *Bioorg. Med. Chem. Lett.* **2** 647
5. Stylianakis I, Kolocouris A, Kolocouris N, Fytas G, Foscolos G B, Padalko E, Neyts J and De Clercq E 2003 *Bioorg. Med. Chem. Lett.* **13** 1699
6. Ilyushina N A, Bovin N V, Webster R G and Govorkova E A 2006 *Antiviral Res.* **70** 121
7. Zoidis G, Fytas C, Papanastasiou I, Foscolos G B, Fytas G, Padalko E, De Clercq E, Naesens L, Neyts J and Kolocouris N 2006 *Bioorg. Med. Chem.* **14** 3341
8. El-Emam A A, Al-Deeb O A, Al-Omar M A and Lehmann J 2004 *Bioorg. Med. Chem.* **12** 5107
9. Protopopova M, Hanrahan C, Nikonenko B, Samala R, Chen P, Gearhart J, Einck L and Nacy C A 2005 *J. Antimicrob. Chemother.* **56** 968
10. El-Emam A A, Al-Tamimi A-M S, Al-Omar M A, Alrashood K A and Habib E E 2013 *Eur. J. Med. Chem.* **68** 96
11. Kadi A A, Al-Abdullah E S, Shehata I A, Habib E E, Ibrahim T M and El-Emam A A 2010 *Eur. J. Med. Chem.* **45** 5006
12. Omar K, Geronikaki A, Zoumpoulakis P, Camoutsis C, Soković M, Ćirić A and Glamoćlija J 2010 *Bioorg. Med. Chem.* **18** 426
13. Kadi A A, El-Brollosy N R, Al-Deeb O A, Habib E E, Ibrahim T M and El-Emam A A 2007 *Eur. J. Med. Chem.* **42** 235
14. Al-Abdullah E S, Asiri H H, Lahsasni S, Habib E E, Ibrahim T M and El-Emam A A 2014 *Drug Des. Dev. Ther.* **8** 505
15. Kouatly O, Geronikaki A, Kamoutsis C, Hadjipavlou-Litina D and Eleftheriou P 2009 *Eur. J. Med. Chem.* **44** 1198
16. Al-Deeb O A, Al-Omar M A, El-Brollosy N R, Habib E E, Ibrahim T M and El-Emam A A 2006 *Arzneim.-Forsch./Drug Res.* **56** 40
17. Almutairi M S, El-Emam A A, El-Brollosy N R, Said-Abdelbaky M and Garcıa-Granda S 2012 *Acta Cryst.* **E68** o2247
18. Shundalau M B, Al-Abdullah E S, Shabunya-Klyachkovskaya E V, Hlinisty A V, Al-Deeb O A, El-Emam A A and Gaponenko S V 2016 *J. Mol. Struct.* **1115** 258
19. Burke K, Werschnik J and Gross E K U 2005 *J. Chem. Phys.* **123** 062206
20. Casida M E 2009 *J. Mol. Struct. (Theochem)* **914** 3
21. Fabian J 2010 *Dyes Pigm.* **84** 36
22. Belletête M, Boudreault P-L T, Leclerc M and Durocher G 2010 *J. Mol. Struct. (Theochem)* **962** 33
23. Iweibo I, Oderinde R A and Faniran J A 1982 *Spectrochim. Acta A* **38** 1
24. Ebata T, Minejima C and Mikami N 2002 *J. Phys. Chem. A* **106** 11070
25. Molina V and Merchan M 2001 *J. Phys. Chem. A* **105** 3745
26. Iikura H, Tsuneda T, Yanai T and Hirao K 2001 *J. Chem. Phys.* **115** 3540
27. Gritsenko O and Baerends E J 2004 *J. Chem. Phys.* **121** 655
28. Duan X-H, Li X-Y, He R-X and Cheng X-M 2005 *J. Chem. Phys.* **122** 084314
29. Maitra N T 2005 *J. Chem. Phys.* **122** 234104
30. Kohn W 1999 *Rev. Mod. Phys.* **71** 1253
31. Jensen F 2007 In *Introduction to Computational Chemistry* 2nd ed. (Chichester: John Wiley)
32. Granovsky A A 2011 *J. Chem. Phys.* **134** 214113
33. Shundalau M B, Pitsevich G A, Malevich E A, Hlinisty A V, Minko A A, Ferber R and Tamanis M 2016 *Comp. Theor. Chem.* **1089** 35
34. Case D A, Darden T A, Cheatham T E, Simmerling C L, Wang J, Duke R E, Luo R, Walker R C, Zhang W, Merz K M, Roberts B, Wang B, Hayik S, Roitberg A, Seabra G, Kolossvai I, Wong K F, Paesani F, Vanicek J, Liu J, Wu X, Brozell S R, Steinbrecher T, Gohlke H, Cai Q, Ye X, Wang J, Hsieh M-J, Cui G, Roe D R, Mathews D H, Seetin M G, Sagui C, Babin V, Luchko T, Gusarov S, Kovalenko A and Kollman P A 2010 In *AMBER 11* (San Francisco: University of California)
35. Wang J, Wolf R M, Caldwell J W, Kollmann P A and Case D A 2004 *J. Comput. Chem.* **25** 1157
36. Berendsen H J C, Postma J P M, van Gunsteren W F, DiNola A and Haak J R 1984 *J. Chem. Phys.* **81** 3684
37. Ryckaert J P, Ciccotti G and Berendsen H J C 1977 *J. Comput. Phys.* **23** 327
38. Essmann U, Perera L, Berkowitz M L, Darden T, Lee H and Pedersen L G 1995 *J. Chem. Phys.* **103** 8577
39. Schmidt M W, Baldridge K K, Boatz J A, Elbert S T, Gordon M S, Jensen J H, Koseki S, Matsunaga N, Nguyen K A, Su S J, Windus T L, Dupuis M and Montgomery J A 1993 *J. Comp. Chem.* **14** 1347
40. http://www.msg.ameslab.gov/GAMESS/GAMESS.html (accessed 13.10.2016)
41. Bode B M and Gordon M S 1998 *J. Mol. Graph. Model.* **16** 133
42. Dunning T H Jr 1989 *J. Chem. Phys.* **90** 1007
43. Becke A D 1993 *J. Chem. Phys.* **98** 5648
44. Lee C, Yang W and Parr R G 1988 *Phys. Rev. B* **37** 785
45. Stephens P J, Devlin F J, Chabalowski C F and Frisch M J 1994 *J. Phys. Chem.* **98** 11623
46. Granovsky A A *Firefly version 8*. http://classic.chem.msu.su/gran/firefly/index.html (accessed 13.10.2016)